Reaction force and surface deformation estimation based on heuristic tissue models

Árpád Takács*§, Tamás Haidegger*§, Imre J. Rudas*

*Antal Bejczy Center for Intelligent Robotics, Óbuda University, Bécsi út 96/b, 1034 Budapest, Hungary
§Austrian Center for Medical Innovation and Technology, Viktor-Kaplan-Strasse 2, 2700 Wiener Neustadt, Austria
E-mail: {arpad.takacs,tamas.haidegger,imre.rudas}@irob.uni-obuda.hu

***Abstract*—In many of the advanced surgical robotic systems, soft tissue mechanics and tool–tissue interaction modeling play an important role in achieving optimal control, relying on model-based control methods. This approach allows one to address crucial issues during teleoperation, such as time-delay, stability or state observation. This paper presents a novel approach for modeling the behavior of soft tissue during surgical interventions, employing the widely-used concept of rheological models. The nonlinear Wiecher model is used for reaction force estimation during tissue indentation, tested on beef liver samples for acquiring mechanical parameters from experimental data. Curve fitting methods have been used in both stress relaxation and constant indentation speed compression phases. Reaction forces are estimated using the proposed model, followed by verification tests on *ex-vivo* beef liver samples. The results of this research showed that the proposed novel rheological soft tissue model is capable of estimating the reaction forces acting on the tool, if the shape of the deformed tissue is known in time.**

I. Introduction

Modern surgical robotic systems require highly accurate and precise tools and control techniques, when we are looking into the development of new control features for master–slave systems. The aim is to achieve superior performance compared to traditional intervention approaches[1]. The modeling of the most basic tissue manipulations (tissue grabbing, indentation and cutting) has therefore gained much attention among the development communities focusing on such systems [2]. In terms of control approach, stable teleoperation requires the knowledge of tissue behavior during manipulation, which primarily depends on its mechanical properties [3]. Precise tool–tissue interaction models would improve the performance of widely-used model-based control approaches, estimating reaction forces and tissue deformation. The required control input of the teleoperation systems (input force, input velocity etc.) can thus be calculated, sending the appropriate commands to the manipulator robotic arm, which will carry out the interventions in an accurate, stable and efficient way [4].

II. Related work

Tool–tissue interaction models are often divided into three distinct groups based on their mathematical and mechanical description [5]:

- *Continuum mechanics-based models*: most of the finite element analysis (FEA) based models represent this group;
- *Heuristic models*: rheological models that are built up from elementary mechanical components, such as springs and viscous dampers;
- *Hybrid models*: a combination of the the two approaches listed above [6].

While continuum mechanics-based tissue models can be very precise in modeling tissue behavior, their application in today's surgical systems is very limited due to the high computational requirements for real-time simulations. On the other hand, heuristic (rheological or mass–spring–damper) models are useful in modeling simple manipulation tasks, mainly uniaxial grabbing or tissue indentation [7]. These models often allow analytical solutions in closed-loop control schemes [8], [9].

There is an extensive literature on reaction force measurement data for constant compression rate indentation [11] and tissue relaxation [10] phases for soft tissues. The mechanical properties of adipose tissues were investigated using linear rheological models during the stress relaxation phase [12]. Yamamoto compared various rheological models during point-to-point palpation for lump detection, although no detailed identification was published on the tissue parameters. An advanced tissue model was proposed in [14] for the identification of soft tissue parameters, which were obtained from experimental data through curve fitting, however, valid results were not achieved. A nonlinear viscoelastic model was proposed by Troyer et al. [15], which was intended for use in hybrid tissue models. However, none of these tissue models were fit to the representation of tissue behavior for both constant compression rate deformation and stress relaxation phases.

III. Rheological soft tissue models

The common properties of rheological soft tissue models have been discussed in details by Wang and Hirai [17], publishing relevant experimental results on the behavior of artificial viscoelastic materials. This paper focuses on one specific family of these models, following

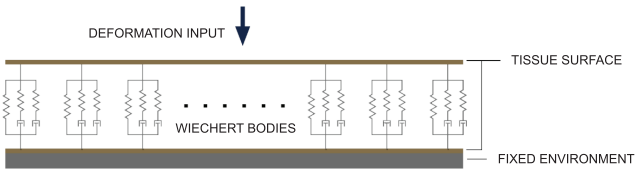

Fig. 1. The tool–tissue interaction proposed in this work, with the distributed Wiechert bodies under the tissue surface.

the concept of Leong et al. [19], considering a uniform distribution of Wiechert bodies under the tissue surface, as shown in Fig. 1. According to this model, the reaction force arising from the tissue deformation can be calculated by the summation of the elementary forces generated by all the distributed elements. The deformation of the tissue surface is assumed to be known at any time. In order to verify the proposed model, the acquired mechanical parameters (spring and damping coefficients) will later be used in non-uniform deformation experiments.

Using rheological models is a simple, pragmatic way for estimating the force response under soft tissue manipulation. Linear or nonlinear spring and damper elements are combined in a parallel or serial manner, representing a behavior similar to that of the tissue when subjected to deformation. The efficient application of this approach requires the knowledge of $u(t)$ deformation function of each of the Wiechert bodies.

There are three commonly used basic models of viscoelasticity in rheological soft tissue modeling: the Kelvin, the Maxwell and the Kelvin–Voigt models. These where explained in details in [8]. Machiraju listed some more complex models in [20], which were based on the combination of the basic models listed above. The serially connected Maxwell and Kelvin bodies form the Maxwell–Kelvin model, used by Leong et al. [19], while the parallel connection of these bodies form the generalized Maxwell model, or its simplest form, the Wiechert model, as shown in Fig. 2. The usage of Wiechert bodies allows one to achieve an accurate and smooth estimation of the tissue behavior, based on 5 mechanical parameters. Considering a linear approach, the transfer function of the Wiechert model in the frequency domain can be written in the following form:

$$F_W(s) = \frac{A_{2_W}s^2 + A_{1_W}s + A_{2_W}}{B_{2_W}s^2 + B_{1_W}s + B_{0_W}}U(s) = W_W(s)U(s), \quad (1)$$

where
$A_{2_W} = b_1b_2(k_0 + k_1 + k_2)$,
$A_{1_W} = (b_1k_2(k_0 + k1) + b_2k_1(k_0 + k_2)$,
$A_{0_W} = k_0k_1k_2b_2$,
$B_{2_W} = b_1b_2$,
$B_{1_W} = b_1k_2 + b_2k_1$,
$B_{0_W} = k_1k_2$.

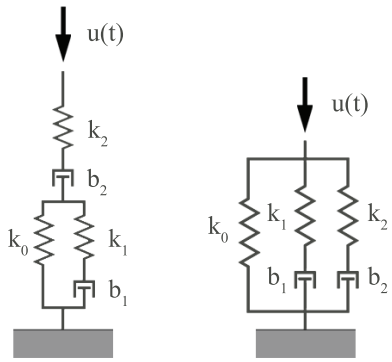

Fig. 2. 5-parameter rheological models of viscoelasticity: the Maxwell–Kelvin model (left) and the Wiechert model (right).

k and b are stiffness and damping coefficients in accordance with Fig. 2.

IV. Experimental setup

In order to obtain the mechanical parameters of the proposed rheological model, 6 pieces of cubic-shaped fresh beef liver tissue samples were deformed, applying a uniform deformation on the tissue surface. The samples were cut to the edge length of 20 mm. Each specimen was deformed at three controlled deformation rates: 20 mm/min, 100 mm/min and 750 mm/min, the latter being the maximum compression rate available on the testing tensile machine, which will be referred to as the near-step input in this paper. The experimental tests were carried out at the Austrian Center for Medical Innovation and Technology (ACMIT), Wiener Neustadt, using a Thümler GmbH TH 2730 tensile testing machine with a direct connection to an Intel Core i5-4570 CPU with 4 GB RAM. The data processing was done using the ZPM 251 (v4.5) software.

The reaction force was measured using an ATI Industrial Automation Nano 17 titanium six-axis Force/Torque transducer, a 9105-IFPS-1 DAQ Interface and power supply, at the sampling time of 62.5 Hz. The data visualization and storage was done on an Intel Core i7-2700 CPU with 8 GB RAM, using the ATICombinedDAQFT .NET software interface. Each specimen was marked by a letter from A to F, as shown in Fig. 3. First, lower indentation speed tests were carried out, the indentation length was 4 mm. In order to achieve uniform deformation, custom-designed 3D-printed flat surface indenter was attached to the the force transducer.

The specimens were compressed at a constant compression rate, however, the nonlinearities from the acceleration and deceleration of the indenter head were filtered out by taking on the first 3.6 mm of the indentation data into account. Each specimen was compressed 12 times at the rates of 20 mm/min and 100 mm/min. During the lower compression rate tests, the reaction force data showed no systematic degradation during the

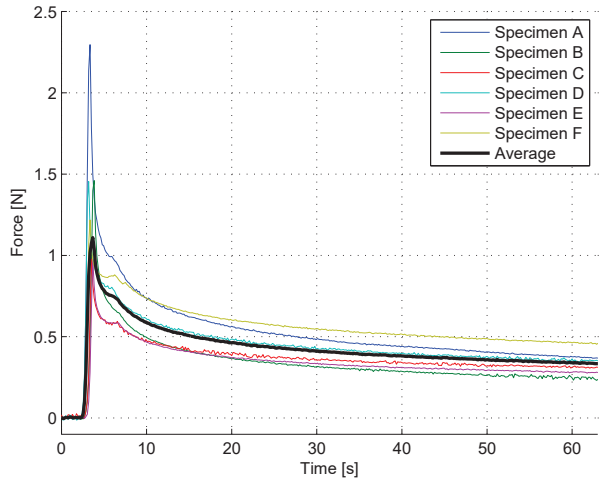

Fig. 3. Reaction force measurement curves for the near-step input relaxation tests.

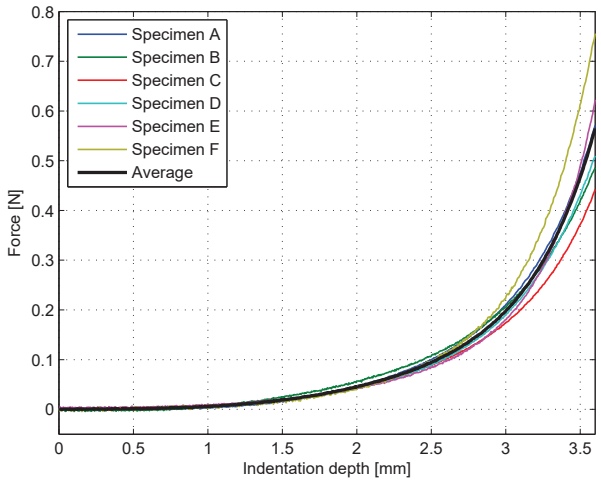

Fig. 4. Reaction force measurement curves for constant compression rate indentation tests at 20 mm/min.

12 indentation cases, which indicated that no substantial tissue damage was caused by these experiments. The compression in the case of the near-step input was done only once, since there was a visible and measurable severe tissue damage after the first such test on each sample.

The force response data for all 6 tissue specimens are displayed in Fig. 3, including the average response curve, normalized to the surface size of 20×20 mm for each specimen. In all cases, a second peak was observed in the measured forces, which occurred at the same time, indicating a systematic measurement disturbance. This peak is most likely the effect of the indenter deceleration and the overshoot of the tensile machine control. This uneven relaxation of the force data does not significantly contribute to the final curve fitting calculations, therefore tis effect was ignored during the initial parameter calculation.

The reaction force measurement curves for the constant compression indentation tests of 20 mm/min and 100 mm/min are shown in Fig. 4 and Fig. 5, respectively. For previously discussed reasons, regarding the nonlinearity of the ramp-input function, only the first 3.6 mm of the indentation depth is considered, visualized on the indentation depth–force diagrams.

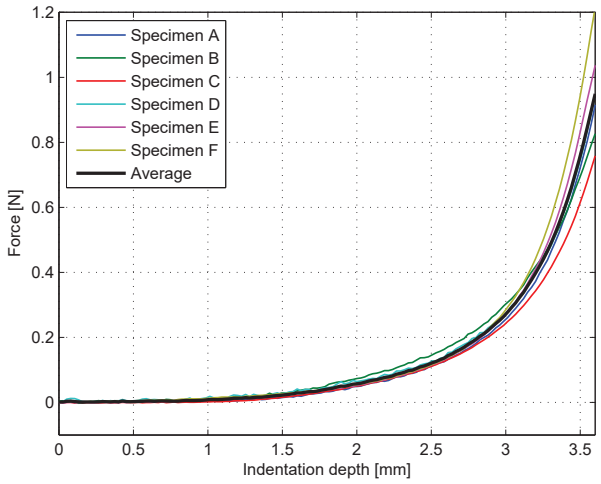

Fig. 5. Reaction force measurement curves for constant compression rate indentation tests at 100 mm/min.

V. Nonlinear mass–spring–damper model

The previous work of Takacs et al. showed that the application of the inverse Laplace transform on (1) is a straightforward way of estimating the tissue parameters of the linear model, using curve fitting on the analytical time-domain force response function [21]. It was also shown that this linear approach fails if the parameter estimation is done using the data from the constant compression rate force response curves. Since the damping parameters are difficult to estimate in engineering practice, a nonlinear model is proposed introducing nonlinearity through the spring elements, using the following stiffness characteristics functions:

$$k_j(\chi_j) = K_j e^{\kappa_j \chi_j} \tag{2}$$

for $j = 0,1,2$, where χ_j is the elongation of the j^{th} spring element. The nonlinear model has 8 mechanical parameters, allowing one to model both tissue relaxation and progressive stiffness characteristics during constant compression rate deformation. The system of differential

equations representing this model is the following:

$$\begin{aligned}\dot{x}_0 &= v(t),\\ \dot{x}_1 &= \frac{1}{b_1}K_1(x_0 - x_1)e^{\kappa_1(x_0-x_1)},\\ \dot{x}_2 &= \frac{1}{b_2}K_2(x_0 - x_2)e^{\kappa_2(x_0-x_2)},\end{aligned} \tag{3}$$

where $v(t)$ is the deformation rate at the indenter tool tip, x_0 is an arbitrary point on the tissue surface. x_1 and x_2 are virtual mass points, which connect the k_1–b_1 and k_2–b_2 elements, respectively. The force output of the system is $F(t)$, which can be written as:

$$\begin{aligned}F(t) = K_0 x_0 e^{\kappa_0 x_0} + +K_1(x_0 - x_1)e^{\kappa_1(x_0-x_1)}\\ + K_2(x_0 - x_2)e^{\kappa_2(x_0-x_2)}.\end{aligned} \tag{4}$$

VI. Model Verification

The nonlinear system of differential equations does not allow analytical solution to this problem, therefore the curve fitting was carried out using the MATLAB R2011a *cftool* toolbox, while the *fminsearch* function was used to find the optimal parameter set, as it was described in [21]. The parameter values for both the linear and nonlinear model cases are listed in Table 1. The optimal set was found by applying curve fitting simultaneously on the datasets corresponding to the near-step input and 20 mm/min constant compression rate test results, while the cost function for *fminsearch* was defined as the sum of the RMS error for each of the curves.

Fig. 6 shows the simulation results for the verification of this approach, where the obtained parameters were fed into the simulated constant compression rate indentation with 100 mm/min. The average RMS error was $\epsilon_{RMSE} = 0.1748$, which was calculated separately for each of the specimens. The simulated and measured force response curves were a good fit to each other. The minor scaling error, which can be observed in Fig. 6 is due to the fact that the parameters were obtained by fitting the force response curve in a 750 mm/min near-step input response, but calculated using the ideal step input compression. This approximation yielded lower stiffness values, as the relaxation already took place during the non-ideal compression.

VII. Non-uniform Surface Deformation

The verification of the proposed model was extended to a non-uniform surface deformation, where additional indentation test were carried out on further specimens. 3 specimens were investigated, having the dimensions of $25 \times 25 \times 200$ mm, cut from the same beef liver sample as the cubic-shaped ones, which lets us assume that the mechanical parameters are identical. These specimens were palpated with a sharp instrument, with an edge length of 30 mm and sharpness of 30°. The indenter was 3D-printed in a way that it created a line-like

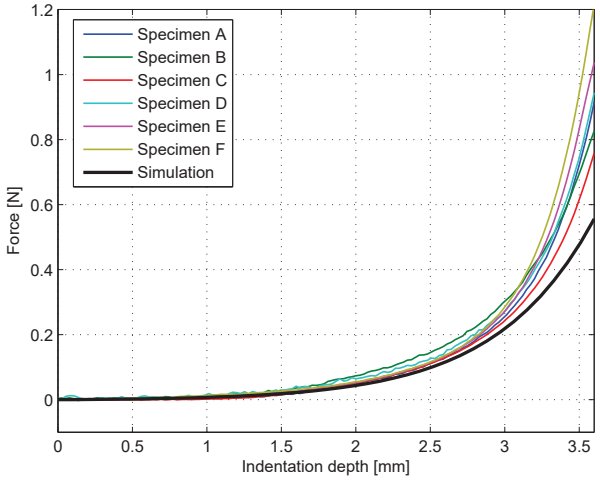

Fig. 6. Reaction force response curves for constant compression rate indentation tests at 100 mm/min. The simulated response of the nonlinear model is also shown, taking the parameters listed in Table 1.

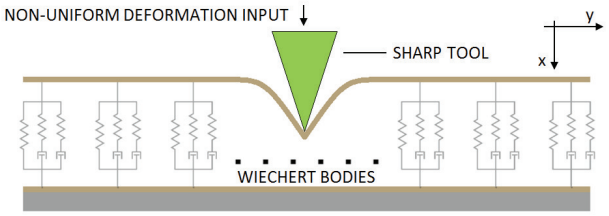

Fig. 7. Non-uniform indentation test schematics, showing the sharp indenter with green color.

deformation input in the specimen surface, perpendicular to the longest dimension (Fig. 7 and Fig. 8). The palpation test were done based on constant compression rate indentations, utilizing 4 different indentation rates: 5 mm/s, 10 mm/s, 20 mm/s and 40 mm/s, compressing the tissue at different points on the surface, reaching the indentation depth of 6 mm.

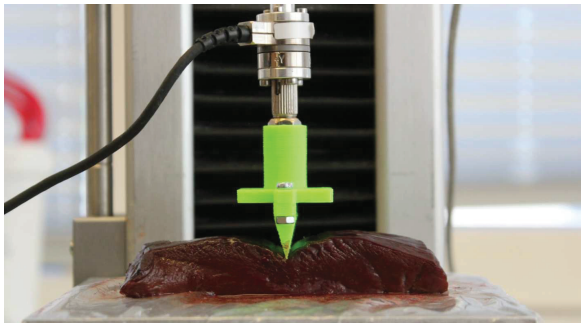

Fig. 8. Experimental setup and tissue deformation during the non-uniform surface deformation tests.

The reaction force estimation was based on three basic assumptions:

TABLE I
TISSUE PARAMETER ESTIMATION RESULTS FROM FORCE RELAXATION AND CONSTANT COMPRESSION RATE TESTS, USING CURVE FITTING.

Model type	K_0 $[N/m]$	K_1 $[N/m]$	K_2 $[N/m]$	b_1 $[Ns/m]$	b_2 $[Ns/m]$	κ_0 $[m^{-1}]$	κ_1 $[m^{-1}]$	κ_2 $[m^{-1}]$	RMSE *combined*
Linear	4.86	57.81	53.32	9987	10464	-	-	-	0.1865
Nonlinear	2.03	0.438	0.102	5073	39.24	909.9	1522	81.18	0.0206

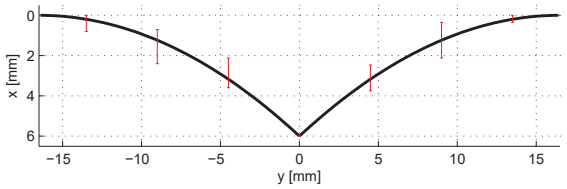

Fig. 9. The surface deformation shape after reaching 6 mm of indentation depth. The red error bars indicate the deviation of the measured position data from the examined surface points. $\rho = 16$ mm.

- like in the previous cases, only the uniaxial deformation component was considered. The horizontal force components were neglected;
- the indentation only affects the tissue surface deformation in a certain ρ distance from the origin, i.e. the indentation point;
- the deformation function is a quadratic approximation of the real deformation function and it is assumed to be uniform along the direction parallel to the line-deformation input axis.

It was also assumed that the resulting reaction force is the sum of the reaction forces appearing on the infinitely small Wiechert bodies:

$$F(t) = \iint_{y,z} f(y,z,t)dydz, \tag{5}$$

where $f(y,z,t)$ is the reaction force of a single element at the (y,z) surface point at time t. The function $f(y,z,t)$ is calculated by solving (17) for each nonlinear Wiechert element. Since each element has a unique deformation rate $v_{x,y}(t)$, *specific* stiffness and damping values can be utilized, which yielded values as shown in Table 2. These values were calculated as the normalization of the mechanical parameters with respect to the surface size of 1 m^2.

In order to carry out numerical simulations, the tissue surface was discretized, dividing it to equally large square elements $A_i = A_{y_i,z_i}$. Each element was given a deformation rate profile $v_i(t)$, which was obtained from video recordings of the experiment. The axis of the camera was fixed on the z-axis, focused on 7 points on the surface moving towards the positive x direction during the indentation. 12 video recordings were analyzed at equally chosen time intervals, allowing one to calculate an average deformation profile. After the processing of the data, it was found that the following function approximates the final deformation shape very well:

$$x(y) = \frac{x_d}{\rho^2}(|y| - \rho)^2, \tag{6}$$

where x_d is the indentation depth. The tissue surface was assumed to be symmetric with respect to the axis of indentation and that the doming effects are neglected:

$$\left.\frac{dx}{dy}\right|_{y=\rho} = 0, \tag{7}$$

These simplifications do not have a significant effect near the indentation point, where the reaction force is assumed to be maximum, and the progressive spring characteristics of the model cause the effect of the points in the farther regions to have a minimal contribution to the resulting reaction force acting on the indenter. The final surface deformation shape is shown in Fig. 9. Error bars are indicating the deviation of the investigated surface points from the estimated surface function. The deformation rate profile $v_i(t)$ at each surface point A_i, can be written as:

$$v(y,t) = \frac{v_{in}}{\rho^2}(|y| - \rho)^2. \tag{8}$$

In the case of the constant rate indentation, the points are moving at a constant speed, which only depends on the distance of the given point from the indentation point. Based on these formulas, (3) was solved for the surface elements and the reaction force values were obtained and summed according to (4). The force response estimation and simulation results for the 3rd specimen at 10 mm/min indentation rate are shown in Fig. 10.

The measured force response values match the estimated ones very well in the initial phase of the indentation. However, at the indentation depth of 4 mm, the slope of the experimental curves abruptly increases, which indicates that a force component has appeared that was unaccounted for until this point. This phenomenon is most likely caused by the lateral tension

TABLE II
SPECIFIC MECHANICAL PARAMETER VALUES, NORMALIZED TO 1 M^2.

K_0^s $[N/m^3]$	K_1^s $[N/m^3]$	K_2^s $[N/m^3]$	b_1^s $[Ns/m^3]$
5075	1095	255	$127{\cdot}10^6$
b_2^s $[Ns/m^3]$	κ_0 $[m^{-1}]$	κ_1 $[m^{-1}]$	κ_2 $[m^{-1}]$
$1.1{\cdot}10^6$	909.9	1522	81.189

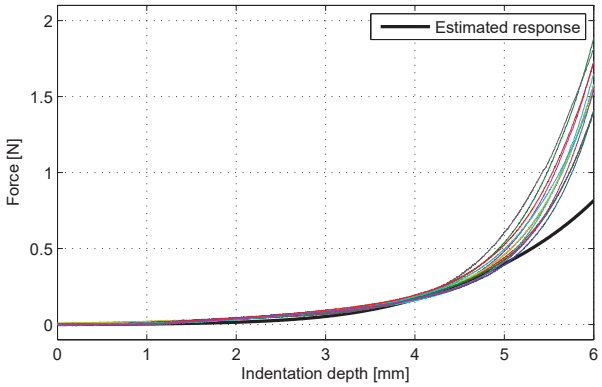

Fig. 10. Experimental results and simulated force response for the case of 10 mm/min indentation for non-uniform surface deformation.

forces, which appear due to the stretching of the tissue surface, which has not been damaged during the experiments. This behavior indicates that the 1 degree of freedom model presented in this paper works sufficiently well in the lower deformation regions, but should be handled with caution in the case of significant lateral tensions.

VIII. Discussion and future work

Rheological tissue models can be used in various forms for the modeling of soft tissue behavior during surgical interventions, representing a simple and straightforward approach for addressing real-time dynamic simulation and force estimation during manipulations. This work proposed and verified a nonlinear rheological model for reaction force estimation during surgical manipulations, assuming that the tissue deformation shape is known. The presented model was verified using experimental results for tissue relaxation and constant compression rate response of *ex vivo* beef liver samples. It was concluded that the estimated reaction force curves gave a good match to the measured values in the case of uniform surface deformation while the model showed an acceptable performance for non-uniform surface deformation tests, based on the idea of uniformly distributed viscoelastic bodies.

Limitations to the approach include the description of the surface deformation function for more complex objects, such as human organs, while the effect of lateral tension forces in large deformations should not be neglected, either. Our future work includes the investigation of these effects and also accounting for the elongation of the tissue surface.

The proposed model is a powerful and useful tool for reaction force estimation for carrying out surgical interventions using blunt instruments (including but not restricted to ultrasound imaging), teleoperation haptic feedback control, surgical simulators etc. Our future work focuses on the model extension to more complex deformations shapes, real-time deformation shape acquisition and model integration into virtual simulators.

IX. Acknowledgment

Tamás Haidegger is a Bolyai Fellow of the Hungarian Academy of Sciences. This work has been supported by ACMIT (Austrian Center for Medical Innovation and Technology), which is funded within the scope of the COMET (Competence Centers for Excellent Technologies) program of the Austrian Government. The research was supported by the Hungarian OTKA PD 116121 grant.

References

[1] A. Takacs, D. A. Nagy, I. J. Rudas, and T. Haidegger, "Origins of surgical robotics: From space to the operating room," *Acta Polytechnica Hungarica*, vol. 13, no. 1, 2016.

[2] M. Hoeckelmann, I. J. Rudas, P. Fiorini, F. Kirchner and T. Haidegger. Current Capabilities and Development Potential in Surgical Robotics. *Int J Adv Robot Syst*, vol. 12, no. 61, pp 1–39, 2015.

[3] T. Haidegger, L. Kovács, R.-E. Precup, B. Benyó, Z. Benyó and S. Preitl, "Simulation and control for telerobots in space medicine," *Acta Astronautica*, vol. 81, no. 1, pp. 390–402, Dec. 2012.

[4] A. Takacs, L. Kovacs, I. J. Rudas, R.-E. Precup, and T. Haidegger, "Models for force control in telesurgical robot systems," *Acta Polytechnica Hungarica*, vol. 12, no. 8, pp. 95–114, 2015.

[5] N. Famaey and J. Vander Sloten, "Soft tissue modelling for applications in virtual surgery and surgical robotics", in *Computer Methods in Biomechanics and Biomedical Engineering*, vol. 11, no. 4, pp 351–366, 2008.

[6] K. J. Parker, "A microchannel flow model for soft tissue elasticity," *Physics in Medicine and Biology*, vol. 59, no. 15, pp. 4443–4457, 2014.

[7] W. Maurel, D. Thalmann, Y. Wu, and N. M. Thalmann, Biomechanical Models for Soft Tissue Simulation. Berlin, Heidelberg: Springer Berlin Heidelberg, 1998.

[8] A. Takacs, S. Jordan, R.-E. Precup, L. Kovacs, J. Tar, I. Rudas and T. Haidegger, "Review of tool–tissue interaction models for robotic surgery applications," in proc. of the *12th IEEE Intl Symp on Applied Machine Intelligence and Informatics (SAMI)*, pp. 339–344. 2014.

[9] A. Takacs, I. Rudas and T. Haidegger. "Surface deformation and reaction force estimation of liver tissue based on a novel nonlinear massspringdamper viscoelastic model." *Medical & biological engineering & computing*, pp. 1–10, 2015.

[10] J. Rosen, J. D. Brown, S. De, M. Sinanan and B. Hannaford, "Biomechanical Properties of Abdominal Organs In Vivo and Postmortem Under Compression Loads," *J Biomech Eng*, vol. 130, no. 2, p. 021020, 2008.

[11] Y. Bao, "A New Hybrid Viscoelastic Soft Tissue Model based on Meshless Method for Haptic Surgical Simulation," *The Open Biomedical Engineering Journal*, vol. 7, no. 1, pp. 116–124, 2013.

[12] N. Alkhouli, J. Mansfield, E. Green, J. Bell, B. Knight, N. Liversedge, J. C. Tham, R. Welbourn, A. C. Shore, K. Kos and C. P. Winlove, "The mechanical properties of human adipose tissues and their relationships to the structure and composition of the extracellular matrix," *American Journal of Physiology - Endocrinology and Metabolism*, vol. 305, no. 12, pp. 1427–1435, 2013.

[13] T. Yamamoto, "Applying Tissue Models in Teleoperated Robot-Assisted Surgery," PhD dissertation, Johns Hopkins University, Baltimore, MD. January, 2011.

[14] F. Leong, "Modelling and analysis of a new integrated radiofrequency ablation and division device," M.Sc. thesis, Dept. of Mechanical Engineering, National University of Singapore, Singapore, 2009.

[15] K. L. Troyer, S. S. Shetye, and C. M. Puttlitz, "Experimental Characterization and Finite Element Implementation of Soft Tissue Nonlinear Viscoelasticity," *J. of Biomechanical Engineering*, vol. 134, no. 11, p. 114501, 2012.

[16] L. Pelyhe and P. Nagy, Relative Visibility of the Diagnostic Catheter. *Acta Polytechnica Hungarica*, vol. 11, no. 10, pp. 79–95, 2014.

[17] Z. Wang and S. Hirai, "Modeling and Parameter Estimation of Rheological Objects for Simultaneous Reproduction of Force and Deformation," in proceedings of the *1st Intl Conf on Applied Bionics and Biomechanics (ICABB-2010)*, Venice, Italy, pp. 1–8, 2010.

[18] X. Wang, J. A. Schoen, and M. E. Rentschler,"A quantitative comparison of soft tissue compressive viscoelastic model accuracy, *J Mech Behav Biomed Mater*, vol. 20, pp. 126–136, Apr. 2013.

[19] F. Leong, W. Huang and C. Chui, "Modelling and analysis of coagulated liver tissue and its interaction with a scalpel blade," *Medical and Biological Engineering Computing*, vol. 51, pp. 687–695, 2013.

[20] C. Machiraju, A.-V. Phan, A. W. Pearsall and S. Madanagopal, Viscoelastic studies of human subscapularis tendon: Relaxation test and a Wiechert model, *Computer Methods and Programs in Biomedicine*, vol. 83, no. 1, pp. 29–33, Jul. 2006.

[21] A. Takacs, P. Galambos, I. J. Rudas and T. Haidegger, "Nonlinear Soft Tissue Models and Force Control for Medical Cyber-Physical Systems," in proc. of the *2015 IEEE Intl Conf on Systems, Man and Cybernetics (SMC2015)*, Hong Kong, 2015, pp. 1520–1525

[22] J. op den Buijs, H. H. G. Hansen, R. G. P. Lopata, C. L. de Korte, and S. Misra, Predicting target displacements using ultrasound elastography and finite element modeling, *IEEE Trans Biomed Eng*, vol. 58, no. 11, pp. 3143–3155, Nov. 2011.